Paper pa02-072
Submitted to the 28th International Conference on High Energy Physics
ICHEP'96, Warsaw, Poland, July 1996

Evolution of Fragmentation Functions and Multiplicity Distributions in ep DIS in the Breit Frame of Reference

H1 Collaboration

Abstract

Data taken in 1994 at the H1 detector at HERA are analysed in the Breit frame of reference. The data are statistically much improved over previously published results from 1993 data. The evolution of the peak and width of the fragmentation function is presented as a function of the four-momentum transfer, Q, of the exchanged photon and compared with e^+e^- results at equivalent centre of mass energies. Discrepancies in the average charged multiplicity disappear as selections are increasingly constrained to give events with hadronic final states in the Breit frame which are more comparable to those of e^+e^- annihilations. Distributions of multiplicity are also presented as a function of Bjorken-x and Q^2, and KNO scaling is tested.

1 Introduction

In a previous publication [1] we have shown the approximate equivalence in terms of hadron production of the ep deep inelastic scattering (DIS) Breit frame of reference to one hemisphere of an e^+e^- annihilation interaction. The equivalent to the centre of mass energy, E^*, is taken to be Q, where $q^2 = -Q^2$ is the square of the four-momentum transferred from the incident lepton. As with the HERA laboraory frames of reference, we choose the positive ('forward') z axis to be in the direction of the incoming proton (target) and exiting spectator system. Polar angles, θ, are measured with respect to this direction in both reference frames. In the Breit frame the incident virtual photon has zero energy, zero transverse momentum and has z component of momentum $-Q$. The negative z direction is thus referred to as the 'current' hemisphere of the interaction. In the context of the naïve quark parton model (QPM) the massless incoming and exiting quark has energy and magnitude of momentum $Q/2$, a fraction of the proton's momentum given by the invariant Bjorken x.

Within QCD, the incident quark will have a higher energy, but since the momentum of the photon is fixed the energy seen in the current hemisphere may be both greater than and less than $Q/2$, as is also the case for $E^*/2$ in any given hemisphere of an e^+e^- interaction. Some of the leading order diagrams, for example final state QCD radiation, have exact parallels between DIS ep and e^+e^- but in other cases, for example initial state QCD radiation, or the boson gluon fusion diagram, there is no e^+e^- equivalent. Note that in leading order of α_s, i.e. two exiting partons as well as the spectator system, DIS events above an incident parton energy of Q can have *no* energy in the current hemisphere other than that due to hadronisation. This is a situation which never exists in any given hemisphere of an e^+e^- interaction.

2 Data selection

In the previous publication the data analysed had incident electrons. The data of 1994, on which this analysis is based, have much higher statistics with incident positrons. The relevant parts of the detector [1, 2] are the same in principle, although the tracking detectors have much improved azimuthal coverage compared with the first analysis. Since the Q^2 values investigated are still far below the kinematic region where anything other than virtual photon exchange is relevant, the results of the two analyses are directly comparable.

The data sample, with basic quality cuts, starts with some 150,000 events, and is then subdivided into two samples, referred to as low ($12 < Q^2 < 80$ GeV^2) and high ($Q^2 > 100$ GeV^2) Q^2, in which the positron energy is well-contained in, respectively, the Backward Electromagnetic Calorimeter and the barrel Liquid Argon Calorimeter. Although many other possibilities have been checked, the calibration errors on the electromagnetic energy scale of these detectors, taken to be $\pm 1\%$ and $\pm 5\%$ respectively, are the dominant sources of systematic error for the results presented in this analysis. Discrepancies in Monte Carlo calculations of acceptance form the next major source and here extremal values are taken as estimates of error. The data are selected to have the scattered positron energy $E'_e > 14$ GeV and to have values of the dimensionless inelasticity variable, $y \sim Q^2/xs$, of $0.05 < y < 0.6$ ensuring negligible contamination from mis-identified photoproduction events. In addition, cuts are placed which safely exclude diffractive events which are not well-modelled with our DIS Monte Carlo programs. The requirement is that there is at least 0.5 GeV deposit of observable energy in the region $4.4° < \theta < 15°$.

Events are then selected in which the quark, according to QPM kinematics, is scattered through $10° < \theta < 150°$, well inside the acceptance of the H1 trackers and thus minimising necessary Monte Carlo corrections. All kinematic variables are calculated using only the scattered lepton which gives both the best resolution in the chosen region and explicit freedom from bias on the hadronic system.

In the analysis of 1993 data a separate correction was made for the effect of QED radiative corrections in so far as a mistaken value of effective Q^2 led to an incorrect multiplicity. There is a further source of error in that a typically overestimated value of Q^2 can also give rise to a miscalculation of the Breit frame axis leading, usually, to an empty current hemisphere. With the new, improved, statistics these have become significant effects. Therefore, to minimise their impact, the new analysis utilises further, more severe, cuts on the mass of the *total* hadronic system, W, of $W^2 > 4400$ GeV^2. Django6 [3] is used in (QED) radiative and non-radiative modes to deal with acceptance as well as remaining radiative problems using bin-by-bin correction techniques. This procedure also removes the small multiplicity contribution from tracks due to decays of short-lived strange particles that are fitted to the *primary* vertex.

Following all of these selection procedures we have 56,213 events in the low Q^2 sample and 5,124 events at high Q^2.

3 Evolution of the Fragmentation Function

The ep Breit frame equivalent of the e$^+$e$^-$ scaled hadron momentum $x_p = 2p_{hadron}/E^*$ is $x_p = 2p_{hadron}/Q$. The event normalised distribution $D(x_p) = (1/N_{evts}) \times dn_{tracks}/dx_p$, the fragmentation function, characterises the processes by which partons shower, and then hadronise. These distributions are shown elsewhere [4]. Typically, at high enough energies and for light enough final state particles, this is an extremely 'soft' function, rising rapidly at small x_p and turning over just before $x_p = 0$. When the fragmentation function is plotted as a function of the variable $\xi = \ln(1/x_p)$ the turn-over region is expanded. According to the expectations of the Modified Leading Logarithmic Approximation (MLLA) and Local Parton Hadron Duality (LPHD), $D(\xi)$ is Gaussian in the neighbourhood of the peak [5].

The higher statistics of this analysis still produce excellent fits to Gaussian distributions and thus confirm this behaviour. To avoid over-dependence on high momentum (low ξ) and low p_t (high ξ) tracks, where most experimental difficulties lie, the fits of this analysis are restricted to the region of $\pm$ one unit of the dimensionless ξ either side of the mean value, but tests in which this area is either decreased or extended show no systematic difference.

The evolution of the fragmentation function may then be effectively summarised by the Q, or E^* dependence of the peak and width values as is shown in Fig. 1. The data have now reached the stage where systematic errors dominate those due to statistics. In this plot they are combined in quadrature. The overall accuracy of the data has improved considerably since the 1993 analysis, but the data are still compatible with the results published earlier, with those of an analysis [6] by the ZEUS collaboration and with various e^+e^- experiments[1], where the relevant evolution variable is the centre of mass energy, E^*.

With the further assumption of gluon coherence MLLA/LPHD predicts [5] the evolution dependence on a dimensionless variable $Y = \ln(Q/\Lambda_{eff})$ where Λ_{eff} sets the scale of the mass of the final state fragmented hadrons. The prediction gives the peak, ξ_{peak} and the width, ξ_{width}, of the Gaussian approximation to be

$$\xi_{peak} = 0.5Y + c_2\sqrt{Y} + O(1)$$

$$\xi_{width} = \sqrt{Y^{\frac{3}{2}}/2c_1}$$

where c_1, c_2 are constants dependent only on the number of colours and flavours within QCD and $O(1)$ contains higher order corrections. The result of a simultaneous fit to the peak and width values obtained from the H1 1994 data alone is shown as a solid line in Fig. 1 and yields the values $\Lambda_{eff} = 0.20 \pm 0.01$ GeV and $O(1) = -0.45 \pm 0.06$, to be compared with the values $\Lambda_{eff} = 0.21 \pm 0.02$ GeV and $O(1) = -0.32 \pm 0.06$ obtained in an analysis [7] of the ξ_{peak} evolution of combined e^+e^- data.

4 The Average Charged Particle Multiplicity

The area underneath the fragmentation function is the average charged multiplicity and this is shown plotted as a function of Q in Fig. 2, again along with the results of the 1993 analysis and with a solid curve which accurately parameterises [8] the average charged multiplicity from many e^+e^- experiments as a function of E^*. The multiplicity error for any given energy to be associated with this fit is at the percent level.

It had already been indicated with 1993 data that, although there was very good agreement between both H1 and ZEUS [6] analyses and those of e^+e^- at high $Q(E^*)$, the DIS analyses give smaller average charged multiplicities at low values. The new data, even after upward corrections for radiative effects, show this to be a very significant effect.

In order to investigate this effect further, we add the four–momenta of all energy clusters in the current region of the Breit frame and plot the resultant total energy, $E_{z<0}$, expressed as a fraction of the event Q, against the corresponding resultant cosine of the Breit frame polar angle, $\cos\Theta_{BF}$, in Fig. 3(a,b) for each of the low and high Q^2 samples. From the discussion in the introduction, it is clear that we would expect that pure QPM events would lie at ($E_{z<0} = Q/2, \cos\Theta_{BF} = -1$) whereas events with an empty current hemisphere and/or with significant initial state QCD radiation would either not appear on this diagram or be spread away from this point. The high Q^2 sample, where α_s is

[1]Published results refer to e^+e^- *events*. As elsewhere in this analysis, track multiplicities from e^+e^- experiments have been reduced by a factor two to correspond to results for each *quark* and a further small reduction has been made to account for K^0 and Λ decay tracks.

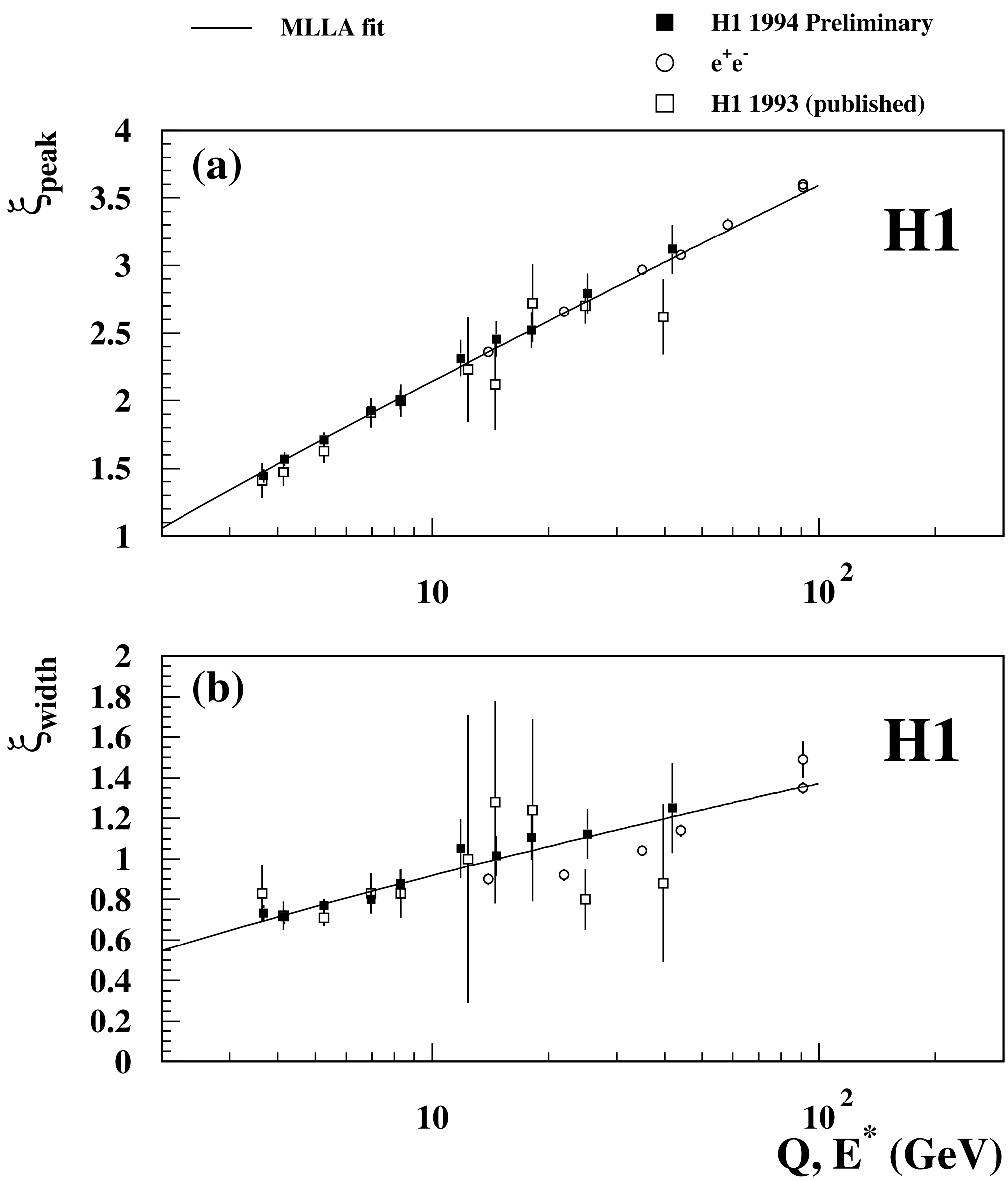

Figure 1: *Evolution of (a) the peak and (b) the width of the fragmentation function as a function of Q compared with e^+e^- results as a function of the centre of mass energy, E^*. The solid line is a fit to MLLA expectations.*

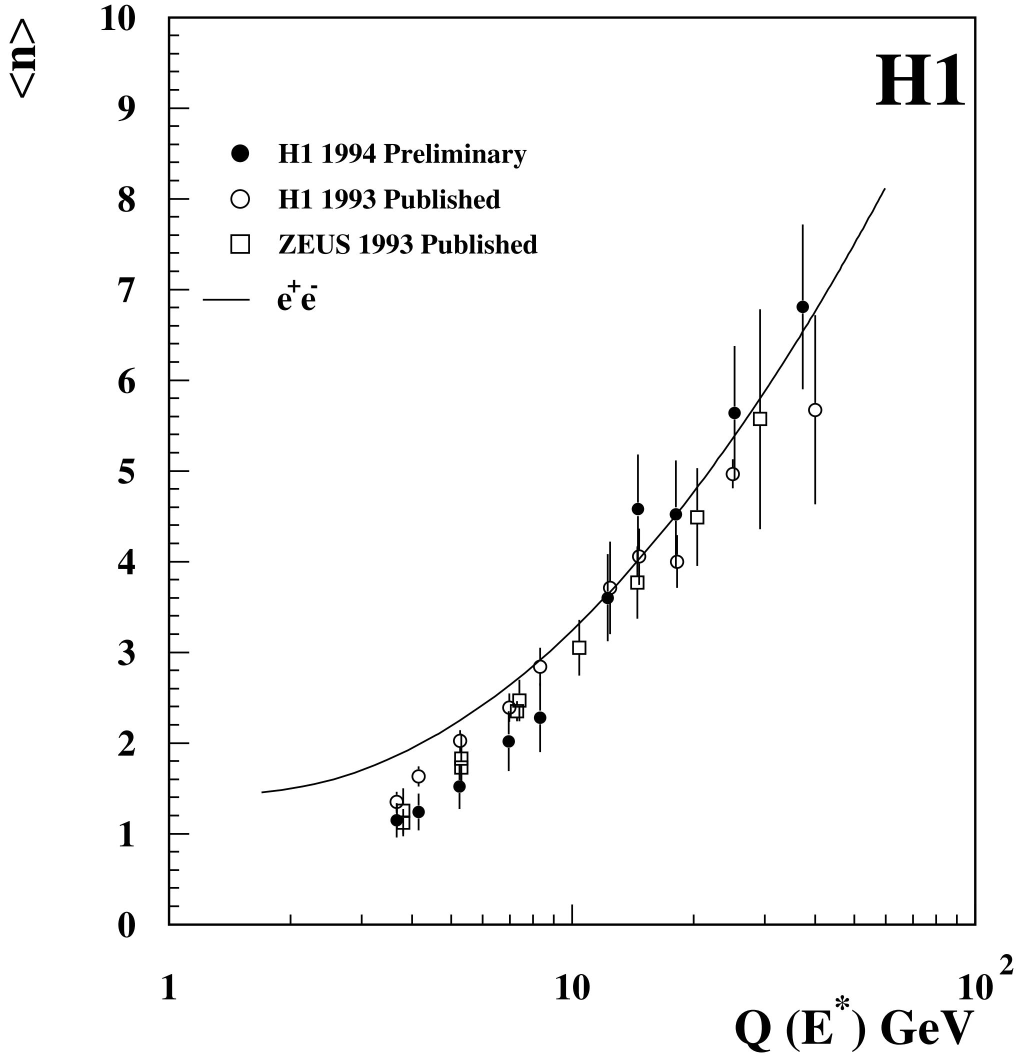

Figure 2: *Average charged multiplicity in the current hemisphere of the Breit frame as a function of Q for this analysis (solid circles) and for the 1993 analysis (open circles). The results from ZEUS 1993 are shown as open square symbols. The curve is a fit to many* e^+e^- *results as a function of the centre of mass energy,* E^*.

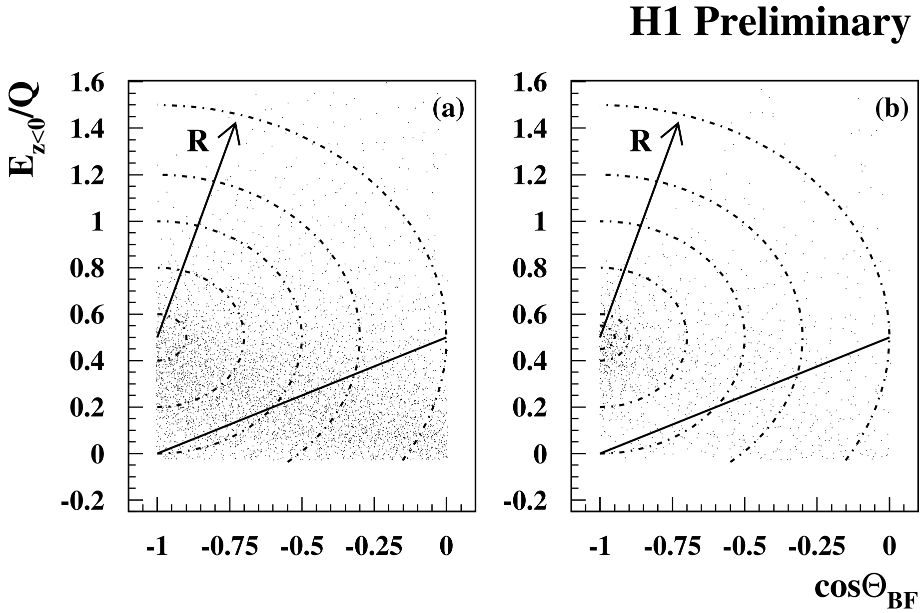

Figure 3: *The total energy of the summed calorimeter cluster four-momentum vectors in the current hemisphere of the Breit frame is plotted as a fraction of the event Q against the polar angle of the resultant vector, for (a) the low Q^2 and (b) the high Q^2 data sample. The annuli define the R variable for Fig. 4 and the solid line indicates the Breit frame energy selection referred to in the text.*

small, indeed shows such a clustering, but this is less evident at low Q^2. Although it is difficult to be very quantitative, it now becomes possible [9] to investigate the effect of selecting ever more 'pure' QPM events by choosing events according to the variable R, where $R^2 = (E_{z<0}/Q - 0.5)^2 + (\cos\Theta_{BF} + 1)^2$. The average multiplicity $\langle n \rangle$ of the events as a function of this variable may be seen with statistical error bars only in Fig. 4(a,b). These results are compared with the average single hemisphere e^+e^- multiplicity evaluated at a value of E^* corresponding to the average value of Q for the relevant H1 sample. The estimates of systematic error on $\langle n \rangle$, which should be interpreted as scale errors on H1 data, are indicated as shaded regions in the neighbourhood of the e^+e^- values. Events with a totally empty current hemisphere, with their zero multiplicity, have no defined value of R and are not included in these plots. However, it may be seen that even without this contribution, as $R \to 0$ the average charged hadronic multiplicity *increases*, possibly even beyond the relevant e^+e^- values, though not now inconsistent with those values considering possible systematic effects. At a more detailed level, there is reason [1] to expect that the democracy in quark flavour production in e^+e^- would lead to a slight ($\sim 3\%$) excess of multiplicity, whilst DIS initial state gluons might give a small excess to ep Breit frame values.

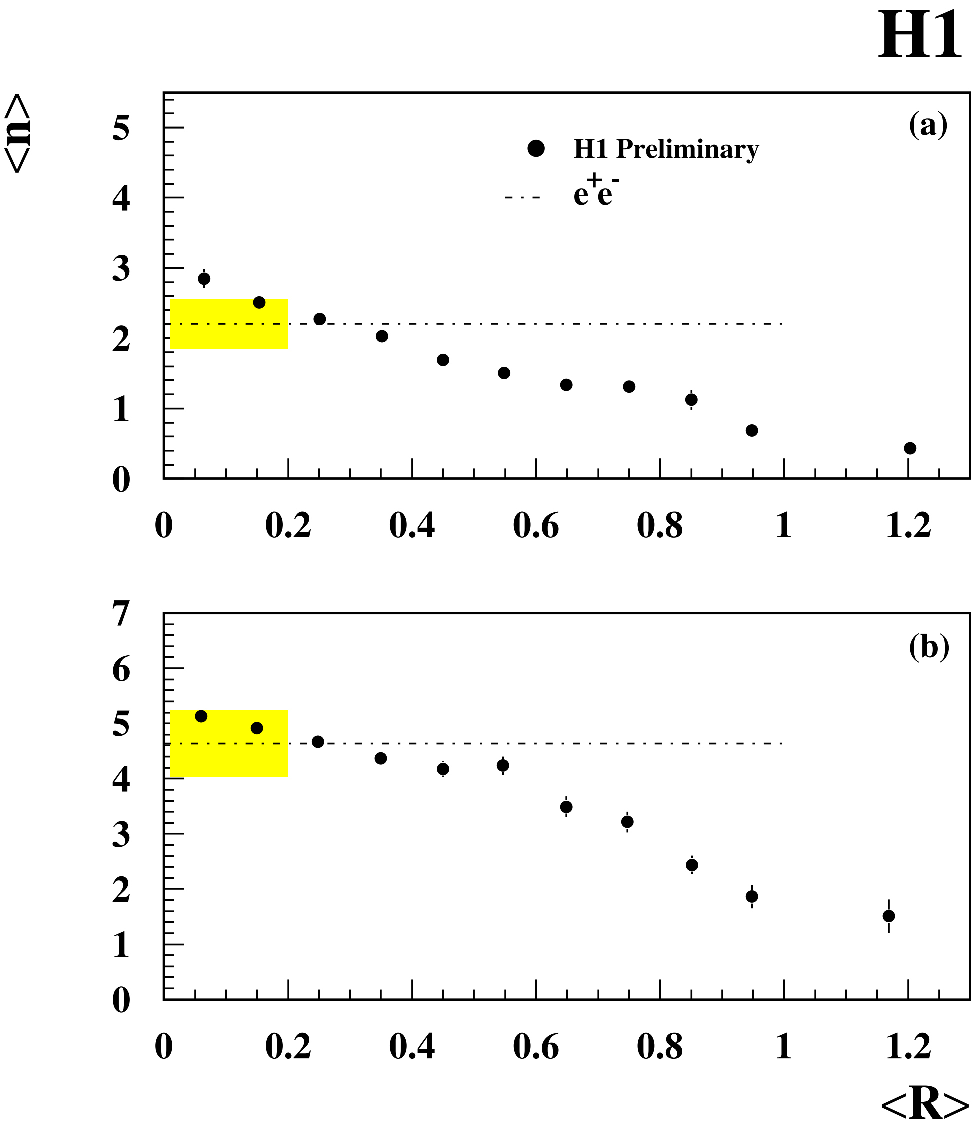

Figure 4: *The average charged multiplicity, shown with statistical error bars only, vs. the radius defined in text and in Fig. 3 for (a) the low Q^2 and (b) the high Q^2 data sample. The solid points indicate H1 data corrected for radiative and acceptance effects but with statistical error bars only. The dashed line shows the equivalent average multiplicity expected for e^+e^- data at a centre of mass energy corresponding to the relevant sample average Q. The shaded regions in the neighbourhood of the e^+e^- values are indicative of the systematic error on the scale of H1 data.*

The above result motivates a cut (shown as a solid line in Fig. 4(a,b) joining the points (-1,0) and (0,0.5) in this plane) to remove extreme low energy and off–axis events. This is termed a Breit frame energy flow selection and produces samples of 25,410 events and 3,752 events at low and high Q^2 respectively which might be thought of as being purer in lowest order events and having average multiplicities closer to those of the equivalent e^+e^- results.

It is interesting to note that the same selection produces minor, but systematically lower in ξ, changes in the peak positions of the fragmentation function with no observable difference in the width. The resulting change to the evolution parameters gives results of $\Lambda_{eff} = 0.22 \pm 0.02$ GeV and $O(1) = -0.40 \pm 0.06$, marginally closer to the e^+e^- values already quoted.

5 Charged Particle Multiplicity Distributions

Charged hadron multiplicity *distributions* are considerably more difficult to measure than average values. In this analysis we have used a number of techniques [10] in going from observed distributions to obtain corrected or 'true' values. In all cases it is straightforward to go in the other direction if it is required to simulate an imperfect apparatus or acceptance. This may be done in a generator-independent manner by forming a generated to reconstructed distribution transfer matrix. This method has been used in order to estimate systematic errors on our various techniques by degrading any given distribution *back* to the 'raw' (simple reconstructed) data level and comparing with the input distribution.

Simple inversion of this matrix to give a true distribution from a raw input distribution is subject to many problems of low statistics of high multiplicity events giving rise to matrix singularities and instabilities. For this reason we have also used a method [11] of transpose approximation to the inverted matrix with successive approximations of reweighting the input Monte Carlo distribution to minimise dependence on the initial generated distribution. In addition, we have again used a simple bin by bin correction procedure and have observed that the larger dependence on the generated distribution, and hence larger systematic error bars in this analysis, is still offset by the ability to get meaningful corrections when the statistics are low. In addition, this is the only method in which it is possible to perform a simultaneous correction for radiative effects back to the Born term.

Using this procedure, the resulting multiplicity distributions are as shown in Fig. 5 with linear and Fig. 6 with logarithmic axes. These results are based on the current hemisphere of *all* events and do not include any energy flow selection. The bins of x and Q^2 are chosen as orthogonal and exclusive but because of the purity cuts used are not totally occupied at the edges of the phase space. This leads to minor discrepancies of average values of x and Q^2 in each bin. In general the observation is that the results are compatible with a gradual shift to higher multiplicities with increasing Q^2 but with the only change as a function of x being due to the minor bin edge effects referred to. It is interesting to note the high values of zero-charged multiplicity events, especially at low Q^2 where we might expect higher order QCD diagrams to dominate. If we integrate over the x dependence in the interests of smaller statistical error bars, and thus greater reach

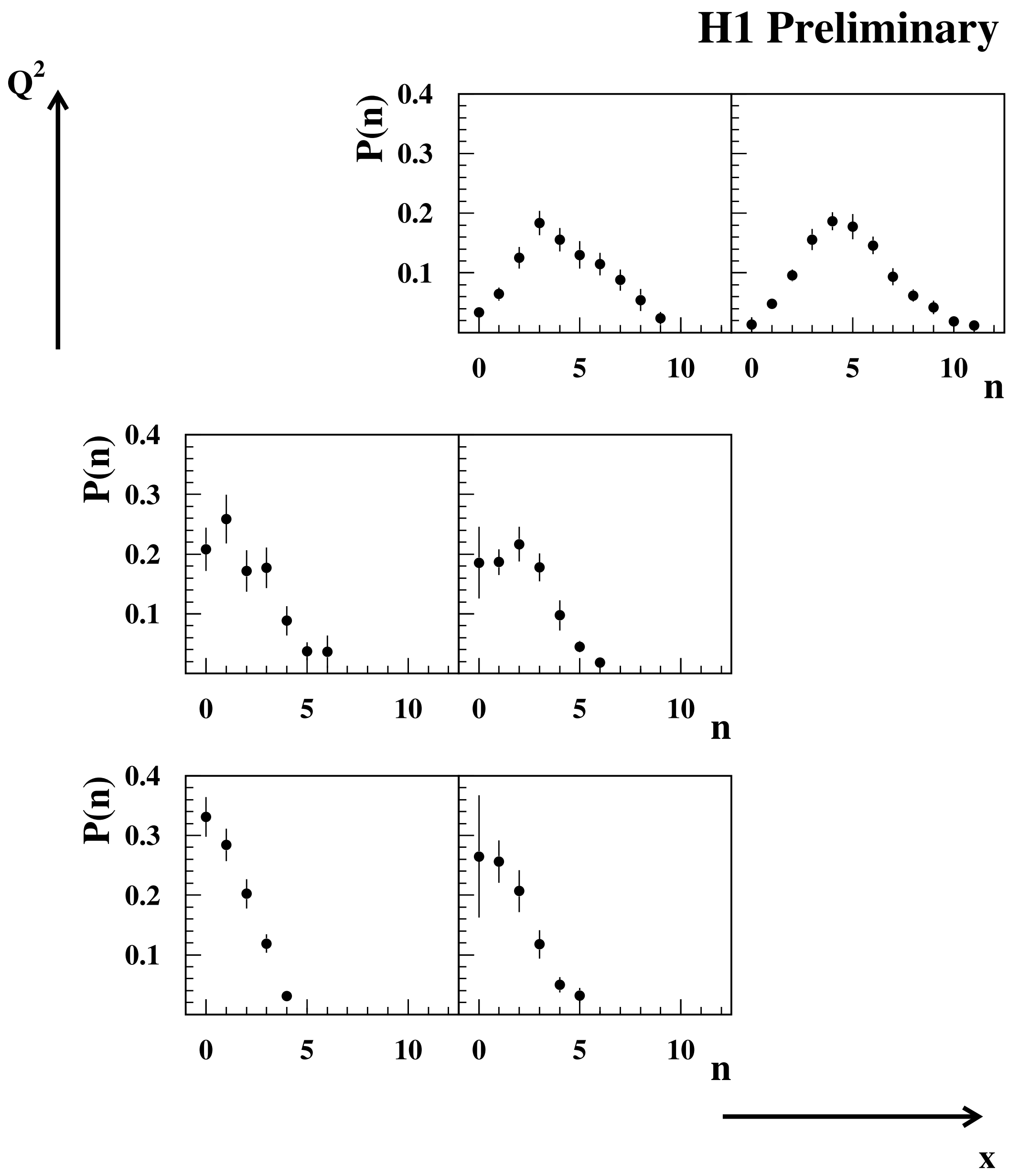

Figure 5: *The event-normalised, corrected, charged hadron multiplicity distributions in the current region of the Breit frame with linear ordinate. Moving from bottom to top the distributions are for* $12 < Q^2 < 30$ GeV^2, $30 < Q^2 < 80$ GeV^2 *and* $200 < Q^2 < 500$ GeV^2 *and from left to right the ranges in Bjorken-x are* $6.10^{-4} < x < 2.10^{-3}$, $2.10^{-3} < x < 1.10^{-2}$ *and* $1.10^{-2} < x < 2.10^{-1}$.

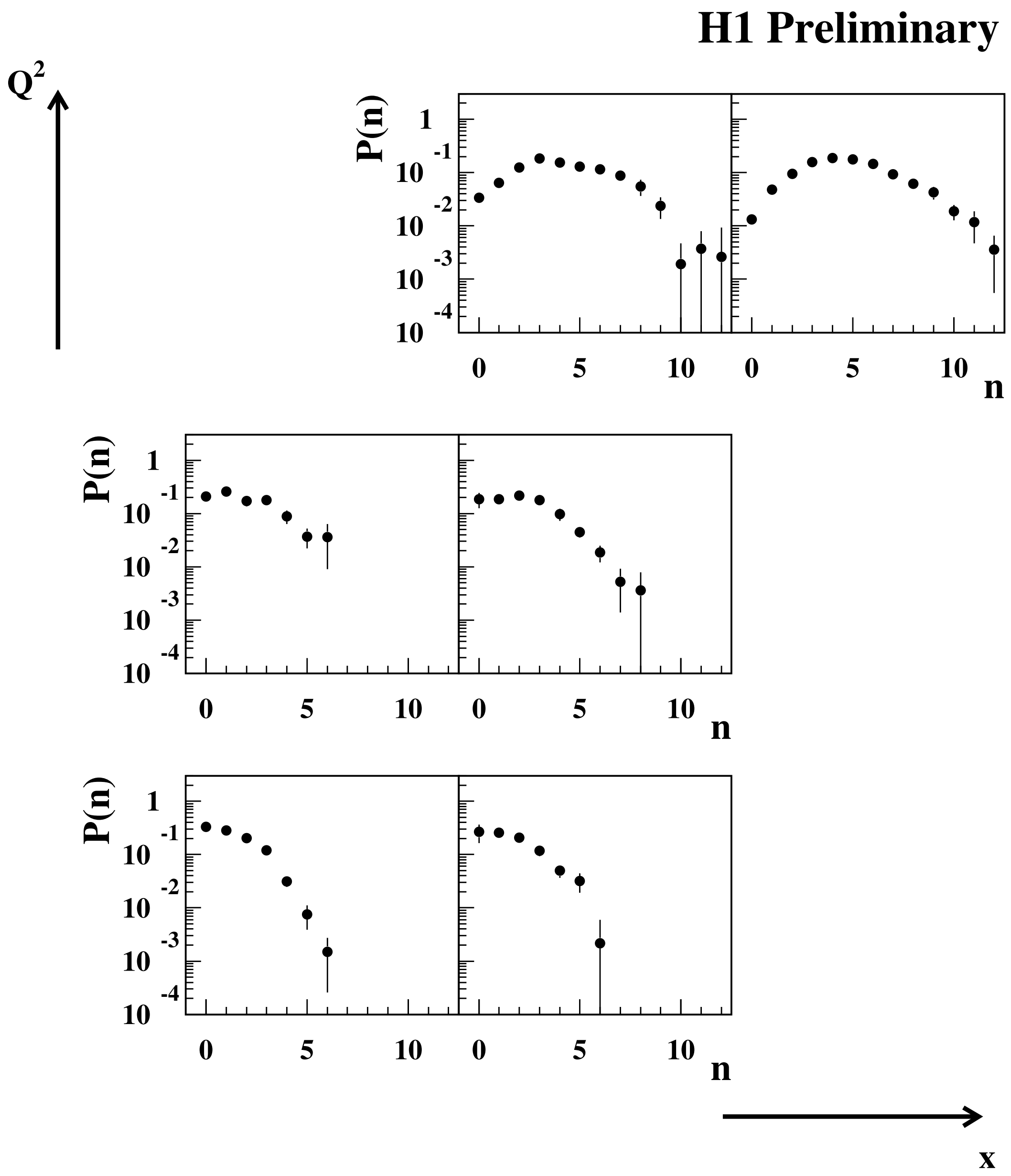

Figure 6: *The event-normalised, corrected charged hadron multiplicity distribution in the current region of the Breit frame with logarithmic ordinate. Moving from bottom to top the distributions are for* $12 < Q^2 < 30$ GeV^2, $30 < Q^2 < 80$ GeV^2 *and* $200 < Q^2 < 500$ GeV^2 *and from left to right the ranges in Bjorken-x are* $6.10^{-4} < x < 2.10^{-3}$, $2.10^{-3} < x < 1.10^{-2}$ *and* $1.10^{-2} < x < 2.10^{-1}$.

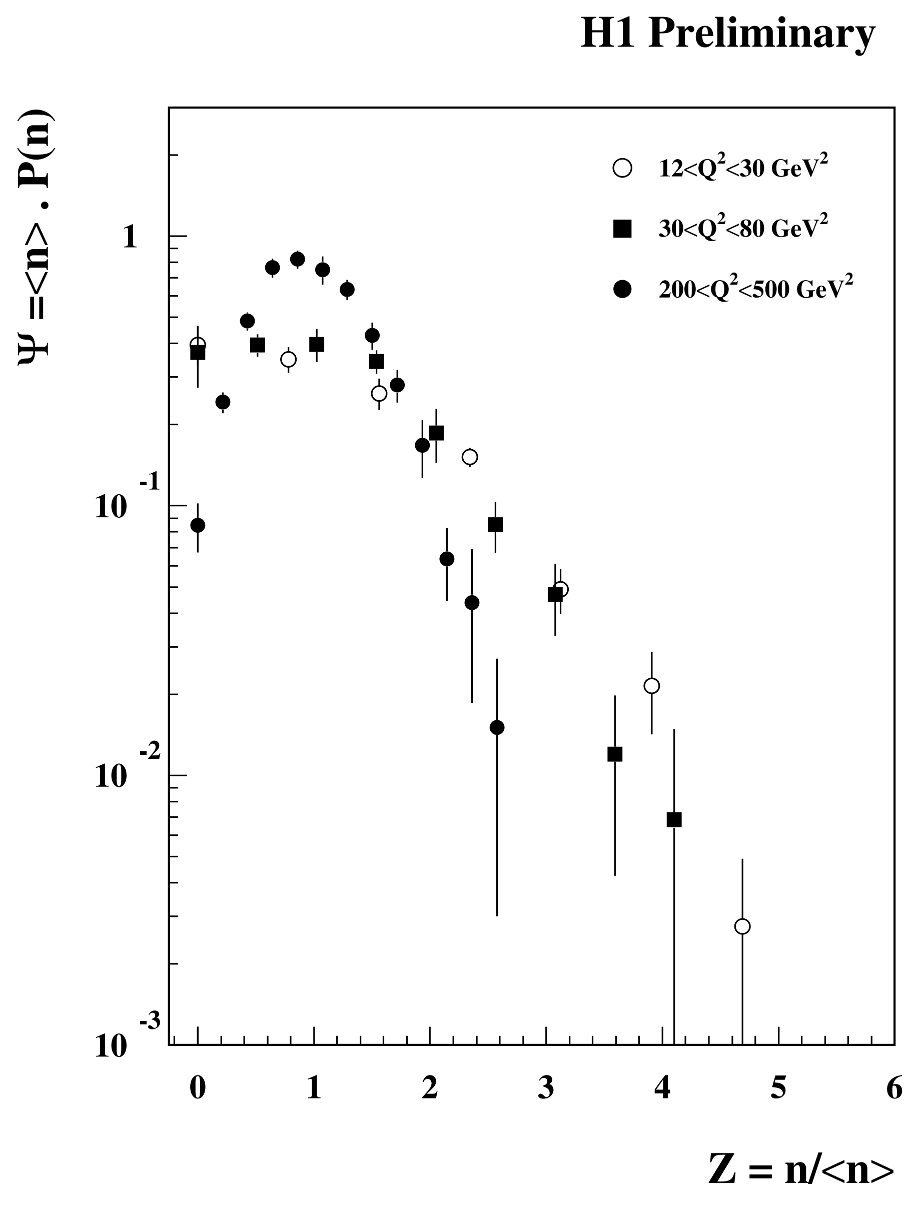

Figure 7: *The charged hadronic multiplicity distribution expressed in terms of the KNO variables for* $12 < Q^2 < 30$ GeV^2 *(open circles),* $30 < Q^2 < 80$ GeV^2 *(squares), and* $200 < Q^2 < 500$ GeV^2 *(solid circles). Statistical and systematic error bars are added in quadrature.*

in multiplicity, the evolution of the shape of the multiplicity distribution, normalised to the average charged hadron multiplicity $\langle n \rangle$, may be found by adopting the KNO [12] quantity $\langle n \rangle \times P(n)$ where $P(n)$ is the probability of observing multiplicity n. The result is shown in Fig. 7. As has been noted by ZEUS [6] and also by H1 [13] in an analysis of multiplicities in the hadronic centre of mass frame, there is clear breaking of KNO scaling in DIS seen by the narrowing of the KNO distribution at high energies. This scaling violation is also seen in Monte Carlo generated events which contain leading order perturbative QCD matrx element calculations.

6 Summary

A 1993 analysis of fragmentation functions in the Breit frame of reference has been repeated with the much higher statistics of 1994 data and is now extended to give multiplicity *distributions* as functions of both x and Q^2. A method of preferentially eliminating the higher order QCD diagrams which do not contribute to e^+e^- interactions shows that some discrepancies between ep Breit frame current hemisphere and e^+e^- average charged multiplicities disappear as conditions are progressively made more comparable. Clear violation of KNO scaling is observed at the highest Q^2 values obtainable.

Acknowledgments

We are grateful to the HERA machine group whose outstanding efforts have made and continue to make this experiment possible. We thank the engineers and technicians for their work in constructing and now maintaining the H1 detector, our funding agencies for financial support, the DESY technical staff for continual assistance, and the DESY directorate for the hospitality which they extend to the non–DESY members of the collaboration.

References

[1] H1 Collaboration, S. Aid et al., Nucl. Phys. 445B (1995) 3.

[2] H1 Collaboration, I. Abt et al., DESY preprint 93-103(1993) and now to be published by Nuclear Instruments and Methods.

[3] G.A. Schuler and H. Spiesberger, Proceedings of the Workshop: Physics at HERA, vol. 3 eds. W. Buchmüller, G. Ingelman, DESY (1992) 1419.

[4] P. Dixon, University of Lancaster thesis, in preparation.

[5] Yu.L. Dokshitzer, V.A. Khoze, A.H. Mueller and S.I. Troyan, "Basics of Perturbative QCD" Editions Frontières (1991); Ya.I. Azimov, Yu.L. Dokshitzer, V.A. Khoze, and S.I. Troyan, Zeit. Phys. C31 (1986) 213, Zeit. Phys. C27 (1985) 65; L.V. Gribov, Yu.L. Dokshitzer, V.A. Khoze, and S.I. Troyan, Phys. Lett. 202B (1988) 276.

[6] ZEUS Collaboration, M. Derrick et al., Zeit. Phys. C67 (1995) 93.

[7] OPAL Collaboration, M.Z. Akrawy et al., Phys. Lett. 247B (1990) 617.

[8] OPAL collaboration, P.D. Acton et al., Zeit. Phys. C53 (1992) 539.

[9] D. Kant, University of London thesis, also published by the Rutherford Appleton laboratory as RAL-TH-96-008.

[10] D. Kant and G. Thompson, H1 note H1-04/96-475.

[11] P. Van Mechelen, University of Antwerp thesis, in preparation.

[12] Z. Koba, H.B. Nielsen and P. Olesen, Nucl. Phys. 40B (1972) 317.

[13] H1 Collaboration, S. Aid et al., paper pa02-075 submitted to this conference.